

Article

Parameter Optimization on the Uniflow Scavenging System of an OP2S-GDI Engine Based on Indicated Mean Effective Pressure (IMEP)

Fu-Kang Ma ¹, Jun Wang ^{1,*}, Yao-Nan Feng ¹, Yan-Gang Zhang ¹, Tie-Xiong Su ¹, Yi Zhang ¹ and Yu-Hang Liu ²

¹ School of Mechanical and Power Engineering, North University of China, Taiyuan 030051, China; mfknu@126.com (F.-K.M.); ncit-feng@nuc.edu.cn (Y.-N.F.); zhangyangang@nuc.edu.cn (Y.-G.Z.); sutiexiong@nuc.edu.cn (T.-X.S.); zhangyi_taiyuan@163.com (Y.-Z.)

² School of Mechanical and Vehicle Engineering, Beijing Institute of Technology, Beijing 100081, China; yuelengfanhua111@163.com

* Correspondence: wjsczq@163.com; Tel.: +86-351-392-2020

Academic Editor: Chang Sik Lee

Received: 20 December 2016; Accepted: 10 March 2017; Published: 15 March 2017

Abstract: In this paper, an opposed-piston two-stroke (OP2S) gasoline direct injection (GDI) engine is introduced and its working principles and scavenging process were analyzed. An optimization function was established to optimize the scavenging system parameters, include intake port height, exhaust port height, intake port circumference ratio, the exhaust port circumference ratio and opposed-piston motion phase difference. The effect of the port height on the effective compression ratio and effective expansion ratio were considered, and indicated mean effective pressure (IMEP) was employed as the optimization objective instead of scavenging efficiency. Orthogonal experiments were employed to reduce the calculation work. The effect of the scavenging parameters on delivery ratio, trapping ratio, scavenging efficiency and indicated thermal efficiency were calculated, and the best parameters were also obtained by the optimization function. The results show that IMEP can be used as the optimization objective in the uniflow scavenging system; intake port height is the main factor to the delivery ratio, while exhaust port height is the main to engine trapping ratio, scavenging efficiency and indicated thermal efficiency; exhaust port height is the most important factor to effect the gas exchange process of OP2S-GDI engine.

Keywords: opposed-piston two-stroke; scavenging process; indicated mean effective pressure (IMEP); optimization

1. Introduction

Pressured by the energy crisis and environmental pollution, the car industry is faced with unprecedented challenges due to its high energy consumption and pollution emissions [1,2]. Over the past two decades, researchers and manufacturers have proposed effective energy-saving and emission reduction methods. Meanwhile, they have focused their study and practice on new types of engines too [3–5]. OP2S engines are different from conventional engines in structure and have better fuel efficiency, power density and balance performance [3]. Opposed-piston engines were conceived in the end of the 19th century in Europe, and subsequently developed in multiple countries for a wide variety of applications including aircraft, ships, tanks, trucks, and so on [3,5–7]. Compared with conventional engines opposed-piston engines have some advantages such as high power density, low heat transfer loss and mean piston velocity, and good balance performance [5]. However, the emission performance is worse because of the high oil consumption. With the

development of suitable emission control technology, however, more and more people are paying increasing attention to the opposed-piston engine concept.

Besides the work done in the 20th century, many other work was done in past 10 years, Hofbauer combined the opposed piston engine and the opposed cylinder engine and proposed the opposed piston opposed cylinder (OPOC) engine for heavy-duty vehicles [3]; Franke has carried performance development work by CAE simulations and testing on the OPOC [7]; Herold has done the thermodynamic analysis to demonstrate the fundamental efficiency advantage of an opposed-piston two-stroke engine over a standard four-stroke engine [5]; Regner used modern analytical tools and engineering methods to develop performance and emissions of an opposed-piston engine [8]; Xu has done numerical analysis of two-stroke free piston engine operating on Homogeneous Charge Compression Ignition (HCCI) combustion [9]; Xu has investigated the effect of the in-cylinder flow on mixture formation and combustion in OPOC engine [10]; Chen used AVL-Fire to simulate the scavenging process of OPOC [11].

For conventional two-stroke gasoline engines, serious loss of fuel short circuit during scavenging process results in poor fuel economy and high emission level. OP2S-GDI engine uses uniflow scavenging and GDI technology to realize separation of the injection and scavenging processes. For GDI engines, the air-fuel mixture is formed in-cylinder, so in-cylinder fluid dynamics play a key role in mixture formation and the combustion process. On the one hand, in order to accelerate air-fuel mixtures, high intensity turbulence is required from a micro perspective. On the other hand, in-cylinder air motion velocity is needed for forming homogenous mixtures from a macro perspective [12]. Swirl, tumble and squish flow are used to form the air-fuel mixtures. For conventional four-stroke GDI engines, in-cylinder flow organization depends on intake duct structure, inlet valve shape, bore-stroke ratio and combustion-chamber shape [13,14]. The injector is installed on the cylinder head. Because injection happens during the intake process, the mixing time is more than sufficient. For OP2S-GDI engines, mixture formation time is short, since the fuel injection process is mainly concentrated in the compression process. Gas motion is unstable during the scavenging and compression processes and breaks down into 3D turbulent motions. Therefore, proper understanding of in-cylinder air motion organization and also the effect of the intake chamber structure and piston configuration are required to improve mixture formation.

The scavenging process is very important for the two-stroke engine, because how much fuel can be effectively burned in the cylinder depends on how much air can be delivered and trapped in the cylinder [3,15–17]. Scavenging system optimization is an effective method to improve the engine performance. For conventional two-stroke engines, the scavenging efficiency was often employed as the optimization objective. However, most two-stroke scavenging systems are “scavenging port-exhaust valve” systems which are different from the “scavenging port-exhaust port” system used on opposed piston two-stroke engines. Compared with “scavenging port-exhaust valve” systems, “scavenging port-exhaust port” systems have a direct effect on the piston expansion stroke, and scavenging efficiency may not describe the scavenging process effect on the indicated thermal efficiency. Hofbauer employed the speed characteristic as the optimization objective in his work [3]. The other studies did not address this point [18]. For the improvement of scavenger efficiency a transient gas exchange simulation was carried out for multiple cases, including two intake port configurations at various back pressures in exhaust system and two port timings [19]. The effects of exhausting back pressure, porting timing and intake port layout on scavenging and trapped air mass in the cylinder were all investigated by transient computational fluid dynamics (CFD) simulation including blow-down and scavenging. By three dimensional (3D) CFD under different intake pressures and engine speeds, Wang et al. evaluated the scavenging process delivery ratio, trapping efficiency, scavenging efficiency and charging efficiency [20]. In addition, the in-cylinder flow motions, which play important roles in controlling the charge mixing and combustion process, were studied for different scavenging port designs. In order to achieve aggressive engine downsizing, a boosted uniflow scavenged direct injection gasoline engine concept has been proposed and researched by means of CFD simulation and demonstration in a single cylinder engine [21].

3D CFD simulations were adopted to evaluate different scavenger port designs for a boosted uniflow scavenged direct injection gasoline engine [20]. Several important design parameters, e.g. scavenging port number, axis inclination angle, swirl orientation angle, scavenging port opening timing, scavenging port height, were investigated in detail under different engine speeds and intake pressures. The effect of valve timing on the gas-exchange process and the subsequent combustion process were investigated on a single cylinder poppet valve GDI engine running in two-stroke engine operation. By individually varying intake and exhaust valve opening and closing timing at low load boundary, middle load and high load boundary of engine operation [22]. A 3D CFD model has been built for the optimization of intake charge organization in order to optimize the 2-stroke uniflow engine performance for vehicle applications. The scavenging process was investigated and the intake port design details were improved [23]. Achates Power has perfected the OP engine architecture, demonstrating substantial breakthroughs in combustion and thermal efficiency after more than 3300 h of dynamometer testing, which is also a good fit for other applications due to its high thermal efficiency, high specific power and low heat rejection [24]. The potential of the 2-stroke concept was applied to range extender engines. The scavenging is of the loop type, without poppet valves, and with a 4-stroke-like lubrication system [25]. In-cylinder flow field analysis in a two-stroke engine under motoring conditions was performed by particle image velocimetry. The engine parameters included engine speed, compression ratio, port area ratio and booster port orientation and the flow parameters [26]. The two-stroke two bank uniflow engine model capability in describing the effect of several parameters on engine performance has been assessed comparing the results of 3D simulations with those of 0D/1D models [27]. A purposely designed 1D model of the engine has been used to compare the performance of the different supercharging systems in terms of power, fuel consumption, and their effect on trapping and scavenging efficiency at different altitudes [28].

In this paper, an optimization function was established to optimize the scavenging system parameters, including intake port height, exhaust port height, intake port circumference ratio, exhaust port circumference ratio and opposed-piston motion phase difference. The IMEP was employed as optimization objective, while at the same time, scavenging efficiency and indicated thermal efficiency were mainly considered too.

2. OP2S-GDI Engine and Scavenging Modeling

2.1. OP2S-GDI Engine Configuration

As shown in Figure 1, the OP2S-GDI engine is equipped with a GDI system and a uniflow scavenging system, and its injector and spark plug are placed on the cylinder liner [29]. On both sides of the cylinder liner there are gas ports – intake ports on one side and exhaust ports on the other side. Intake ports are used to deliver fresh air into the cylinder, and exhaust ports are used to remove burnt gas from cylinder. In the working process, the piston motion controls the opening and closing of the ports. There are two pistons placed in the cylinder liner, and a combustion chamber is formed when the two pistons move to the closest position. The piston which controls the opening and closing of intake air ports is defined as the intake piston and the piston which controls the opening and closing of the exhaust air ports is defined as the exhaust piston. When the distance between the two pistons is minimized, it is defined as the inner dead center (IDC); when the distance between the two pistons is maximized, it is defined as the outer dead center (ODC). The structure parameters are listed in Table 1.

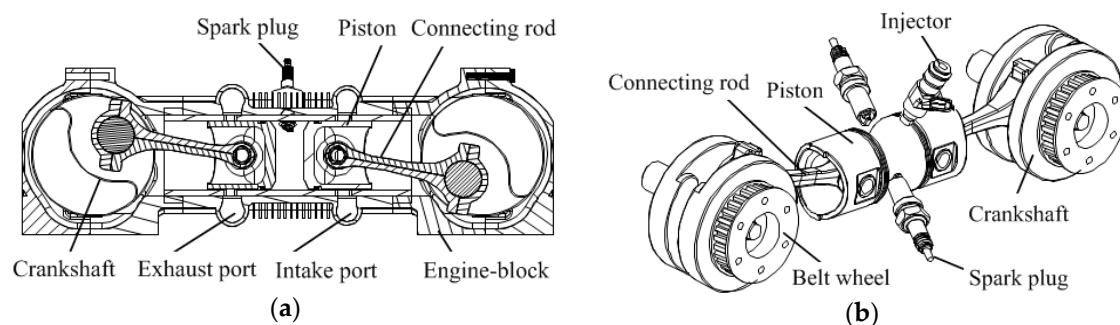


Figure 1. Configuration of OP2S gasoline engine (a) Section of OP2S gasoline engine; (b) Opposed crank-connecting rod mechanism.

Table 1. Engine specifications.

Parameters	Unit	Value
Bore	mm	56
Stroke	mm	49.5 (×2)
Connecting rod	mm	82.5
Effective compression Ratio	—	10.5
Engine speed	rpm	6000
Number of intake ports	—	10
Number of exhaust ports	—	10
Intake port height	mm	12
Exhaust port height	mm	14
Intake port circumference ratio	—	0.75
Exhaust port circumference ratio	—	0.6
Intake port radial angle	°	15
Exhaust port radial angle	°	0
Opposed-piston motion phase difference	°CA	17
Power	kW	15
Fuel consumption rate	g/kW·h	276

2.2. Key Parameters and Uniflow Scavenge System

This research examines key factors: intake port height (h_i), exhaust port height (h_e), intake port width (d_i), exhaust port width (d_e) and the opposed-piston motion phase difference (ϕ), as shown in Figures 2 and 3 [29,30]. Port height stroke ratio (α) and circumference ratio (β) are the two main influencing factors in the OP2S-GDI engine scavenging process. The α is defined as the ratio of port height and stroke length; the β is defined as the ratio of port width and cylinder circumferential length. The ϕ is between the intake piston and exhaust piston motion phase difference. It should be noted that the port timing is asymmetric, whereby the exhaust ports open earlier than the intake ports; at the same time, and the exhaust ports also close earlier than the intake ports. The discharge period up to the time of the scavenging port opening is called the free exhaust period. The intake port close after the exhaust port close, since the flow toward the intake port continuously, additional fresh air is obtained. The additional air inflow period up to the time of intake port close is called the post intake period. Due to opposed-piston motion phase difference, opposed pistons on both sides can not arrive at each top dead center (TDC) simultaneously.

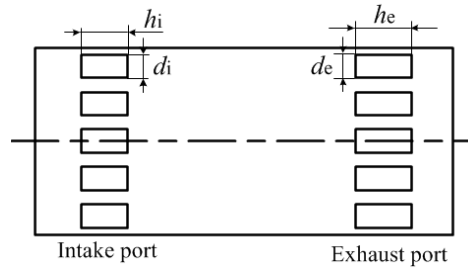


Figure 2. The port parameters.

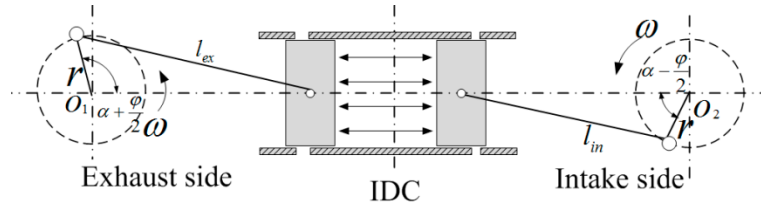


Figure 3. Opposed crank-connecting rod mechanism.

If the phase difference of the intake and exhaust piston is ϕ , the relative displacement of opposed-piston should be known by the kinematics of traditional crank-connecting rod mechanism [31].

2.3. Scavenging Process Modeling

2.3.1. Working Process One-Dimensional Model

Based on the hypothesis of one dimensional isentropic flow, the fluid flow condition of free exhaust process can be written as supercritical condition:

$$\frac{dm_s}{d\phi} = \frac{C_v F_s}{6n} \sqrt{\frac{2gk}{(k-1)RT}} \cdot p_z \cdot \left(\frac{2}{p_z + 1}\right)^{\frac{1}{k-1}} \quad (1)$$

The fluid flow condition of scavenging process can be written as subcritical conditions:

$$\frac{dm_s}{d\phi} = \frac{C_v F_s}{6n} \sqrt{\frac{2gk}{k-1}} \cdot \frac{p_s}{\sqrt{RT}} \cdot \sqrt{\left(\frac{p_z}{p_s}\right)^{\frac{2}{k}} - \left(\frac{p_z}{p_s}\right)^{\frac{k+1}{k}}} \quad (2)$$

where C_v is the intake or exhaust port flow coefficient, n is the engine speed, p_s is the inlet pressure, p_z is the outlet pressure. For the exhaust ports, p_s is the in-cylinder pressure and p_z is the exhaust chamber pressure; for the intake ports, p_s is the intake chamber pressure and p_z is the in-cylinder pressure. F_s is the area of the intake or exhaust ports at different crank angles, g is the gravitational acceleration, k is the adiabatic exponent, R is the gas constant, T is the gas temperature.

The unflow scavenging process is assumed to be completed in three models: perfect displacement model, perfect mixing model and short circuit model. In practice, the scavenging process includes multiple scavenging models, giving a relation for scavenging efficiency [32]:

$$\eta_{sc} = \begin{cases} l_0 & l_0 \leq l_{0c} \\ 1 - e^{-i \cdot l_0} & l_0 > l_{0c} \end{cases} \quad (3)$$

where the term i is the scavenging model index, l_{0c} is the demarcation point between perfect scavenging and rich exhaust scavenging.

Section 2.3.3 shows the scavenging profile which was calculated by the 3D simulation as the input boundary conditions of 1D simulation scavenging model [33]. Simulation modes based on GT-Power were established, and Wiebe mode was used to describe the combustion process in the cylinder, and Woschni mode was used to calculate the heat transfer in the cylinder. The relationship

of residual gas coefficients between the exhaust and residual gas coefficients in the cylinder is employed to describe the two-stroke scavenging process.

2.3.2. Scavenging Process Three-Dimensional CFD Model

AVL-Fire software is used to build CFD model in the working process simulation. Fame Engine plus is used to generate the cylinder moving meshes by defining moving selection, buffer selection, interpolation selection and the relative motion rule of the opposed-piston. Intake and exhaust chambers generate the no-movement meshes which are refined near the intake and exhaust ports, in order to capture the significant flow gradients accurately, as shown in Figure 4. The full-scale three-dimensional CFD model consists of 249,528 cells for the scavenging process and 47,961 cells for the compression process after rezoning. The dynamic mesh of the piston motion in the intake and exhaust strokes has been treated according to the realistic motion rule of opposed pistons. The scavenging calculation is from exhaust port opening (EPO) to intake ports closing (IPC), while the in-cylinder working process is from IPC to EPO. Mesh movement including three parts—intake and exhaust piston and cylinder—was used to simulate the gas motion during the entire working process model in the calculation of turbulence.

The boundary conditions were chosen to reflect the physical conditions in the validation model and the prototype engine. The EGR ratio represents the percentage of the burned gas. The $K-\zeta-f$ model is employed to capture turbulence. The time step for the calculation is set about 0.5° . A constant pressure boundary condition is used for both intake and exhaust ports. Mean scavenging pressure is taken as 1.2 bar and mean exhaust receiver pressure is taken as 1 bar. Frictional effects at the walls are not taken into account, i.e., the smooth wall option is used for turbulent flow boundary conditions. The initial conditions in the cylinder for every scheme are extracted from the GT-Power software simulation. The flow field is initialized by specifying the temperature, pressure and turbulence intensity. By performance prediction, the initial pressure and temperature in the cylinder are computed in a scheme of 15 kW at an engine speed of 6000 rpm, which are the initial conditions for CFD. Initial temperatures of cylinder, intake chamber and exhaust chamber are given a value of 788 K, 322 K, and 634 K, respectively.

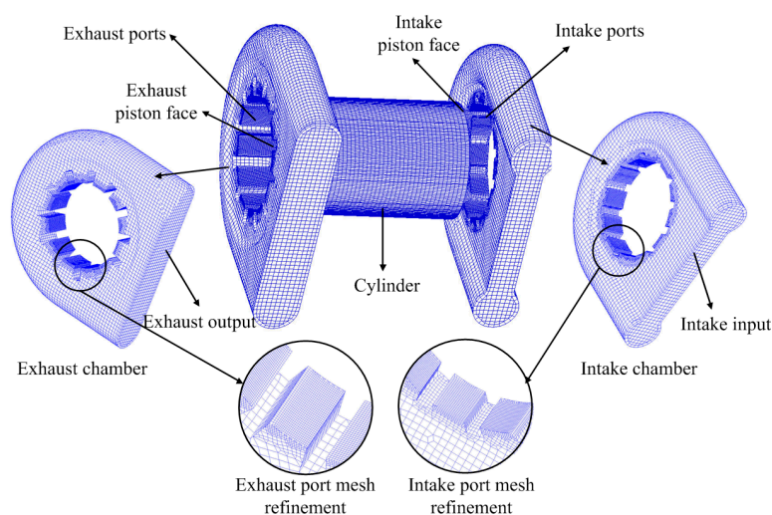


Figure 4. CFD calculation model.

In order to investigate mesh independence, two additional meshes are tested. One with approximately 150,000 cells denoted “coarse” and one with approximately 237,000 cells denoted as “medium”. The reference mesh of 304,000 cells is referred to as “fine” [34]. The effect of mesh resolution is presented by comparing radial profiles of tangential velocity as shown in Figure 5.

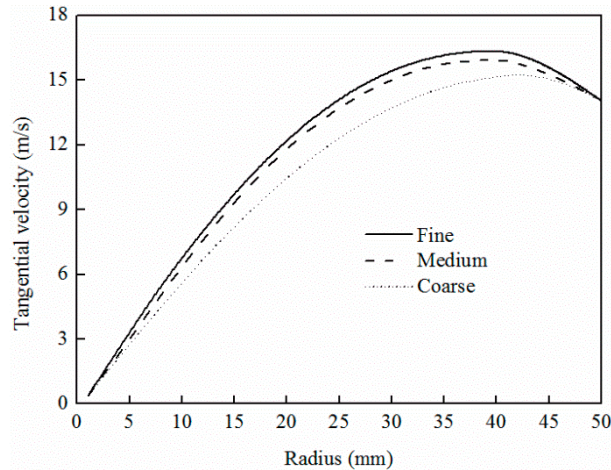


Figure 5. Comparison between different mesh resolutions.

The profiles are sampled the cross section of cylinder center when the opposed piston is at the ODC. The comparison shows that the velocity profiles are in good agreement and the medium mesh can be used as the working mesh.

2.3.3. Scavenging Curve

Before exhaust port opening, the in-cylinder burnt gas is defined as the gas mixture which is made up of H_2O , CO_2 and N_2 . As shown in Figure 6a, the ratio of in-cylinder burnt gas composition remains unchanged during the free exhaust phase. During the early stages of the scavenging process, the composition of H_2O and CO_2 are decreased but the composition of O_2 is increased. Because the proportion of N_2 in the fresh charge is greater than in the burnt gas, the composition of N_2 is increased slightly. During the middle and later stages of the scavenging process, the in-cylinder N_2 and O_2 compositions remain unchanged because the CO_2 and H_2O are completely expelled from the cylinder. As shown in Figure 6b, the ratio of gas compositions in the exhaust chamber has the same change trend as the in-cylinder gas compositions. The primary difference is that variation of gas compositions in exhaust chamber lagged behind that of gas compositions in cylinder by $40^\circ CA$. When the ratio of gas compositions in the exhaust chamber is changed, a fresh charge is short-circuited in the scavenging process.

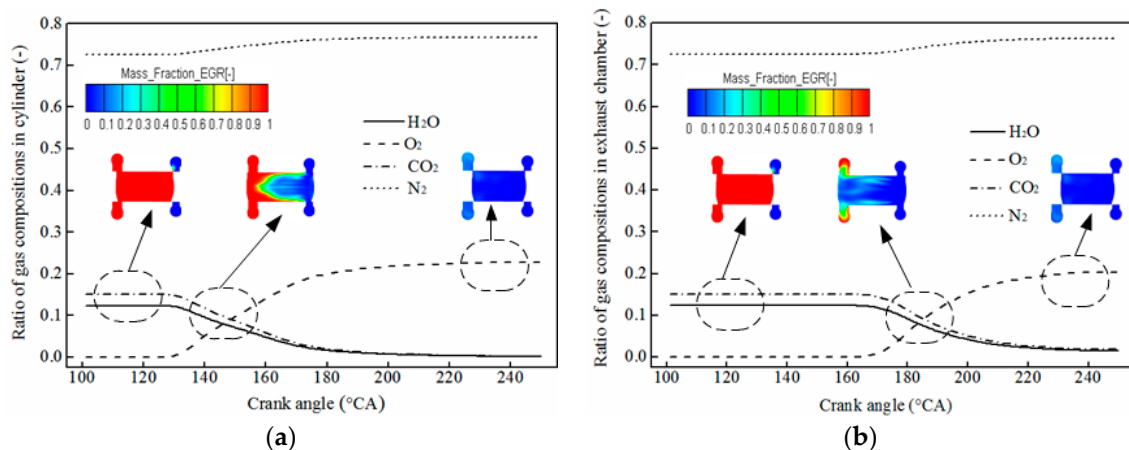


Figure 6. The variation of gas components in the scavenging process: (a) In-cylinder gas components; (b) Exhaust chamber gas components.

Through the analysis above, the state parameters of the scavenging process can be obtained by calculating the change of fresh charge (O_2 and N_2). The residual gas coefficient in cylinder is described with O_2 and N_2 in cylinder as follows:

$$\eta_{R,cyl} = 1 - \frac{O_{2,cyl} \% + \frac{76.8\%}{23.2\%} O_{2,cyl} \%}{O_{2,cyl} \% + N_{2,cyl} \% + CO_{2,cyl} \% + H_2O_{2,cyl} \%} \quad (4)$$

where $O_{2,cyl}\%$, $N_{2,cyl}\%$, $CO_{2,cyl}\%$ and $H_2O_{2,cyl}\%$ is the instantaneous mass percent of O_2 , N_2 , CO_2 and H_2O in the cylinder.

The residual gas coefficient in the exhaust is described by the O_2 and N_2 in the exhaust as follows:

$$\eta_{R,exh} = 1 - \frac{O_{2,exh} \% + \frac{76.8\%}{23.2\%} O_{2,exh} \%}{O_{2,exh} \% + N_{2,exh} \% + CO_{2,exh} \% + H_2O_{exh} \%} \quad (5)$$

where $O_{2,exh}\%$, $N_{2,exh}\%$, $CO_{2,exh}\%$ and $H_2O_{exh}\%$ are the instantaneous mass percentages of O_2 , N_2 , CO_2 and H_2O in the exhaust.

As shown in Figure 7, the profile should be analyzed from 1.0 to zero. Before the intake port opens, no fresh charge passes into the cylinder. Both the cylinder residual ratio and exhaust chamber residual ratio remain at 1. With the outward movement of pistons, the intake and exhaust ports are unsealed, and a fresh charge flows into the cylinder. The burned gas is constantly replaced by a fresh charge. When the cylinder residual ratio is 0.35, the synthetic scavenging profile begins to decline obviously. Through the whole process, the OP2S-GDI engine scavenging profile remains above the perfect mixing curve which means the scavenging process of the OP2S-GDI engine is satisfactory. This profile will be used as the boundary condition of our 1D simulation to calculate the OP2S-GDI engine scavenging efficiency and trapping efficiency.

A simulation running at 20% load of 1200 rpm is performed and a series of comparison validations of the 1D in-cylinder working process, 3D scavenging process and motoring conditions were conducted, as shown in Figure 8. The simulation results agreed with the experimental results in the scavenging process, which indicates that the parameters were reasonably selected.

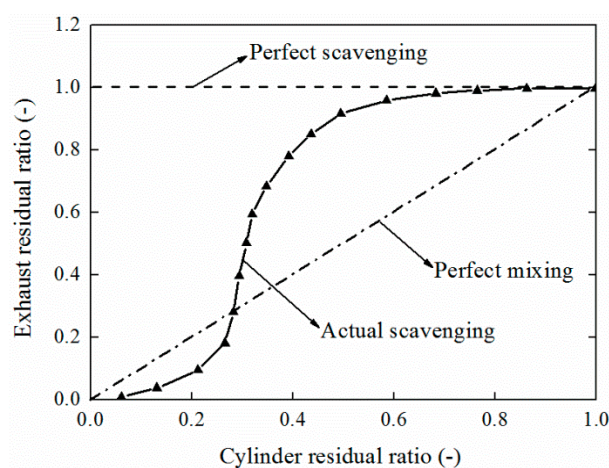


Figure 7. The uniflow scavenging profile.

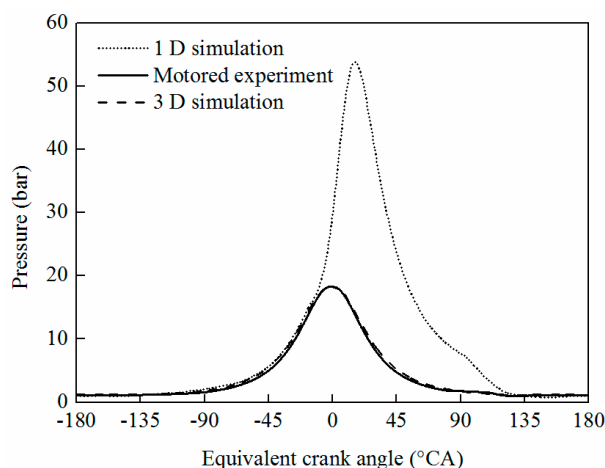


Figure 8. In-cylinder pressure comparison.

3. Results and Discussion

3.1. Scavenging Characteristics

Delivery ratio, trapping efficiency and scavenging efficiency were usually employed as evaluation index on the two-stroke scavenging system.

The delivery ratio:

$$l_0 = \frac{\text{mass of delivered air (or mixture) per cycle}}{\text{reference mass}} \quad (6)$$

The reference mass is defined as displaced volume \times ambient air (or mixture). Ambient air (or mixture) density is determined at atmospheric conditions or at intake conditions.

The trapping efficiency:

$$\eta_{tr} = \frac{\text{mass of delivered air (or mixture) retained}}{\text{mass of delivered air (or mixture)}} \quad (7)$$

The trapping efficiency indicates what fraction of the air (or mixture) supplied to the cylinder is retained in the cylinder.

The scavenging efficiency:

$$\eta_{sc} = \frac{\text{mass of delivered air (or mixture) retained}}{\text{mass of trapped cylinder charge}} \quad (8)$$

The scavenging efficiency indicates to what extent the residual gases in the cylinder have been replaced with fresh air.

When the reference mass in the definition of delivery ratio is trapped cylinder mass (or closely approximated by it) then [33]:

$$\eta_{sc} = l_0 \cdot \eta_{tr} \quad (9)$$

For the perfect displacement model, trapping and scavenging efficiency vary with delivery ratio as follows:

$$\begin{aligned} \eta_{tr} &= 1 & \eta_{sc} &= l_0 & \text{for } l_0 \leq 1 \\ \eta_{tr} &= 1/l_0 & \eta_{sc} &= 1 & \text{for } l_0 > 1 \end{aligned} \quad (10)$$

For the perfect mixing model, trapping and scavenging efficiency vary with delivery ratio as follows:

$$\eta_{tr} = \frac{1}{l_0} \cdot (1 - e^{-l_0})$$

$$\eta_{sc} = 1 - e^{-l_0}$$
(11)

3.2. Parameter Optimization

3.2.1. Analysis of Simulation Results

For the OP2S-GDI engine, the h_i , h_e and ϕ are the main decision factors on intake and exhaust port time and gas exchange time. Figure 9a shows the effect of the h_i and β_i on delivery ratio. Delivery ratio increases with the raise of the h_i , because higher h_i results in earlier IPO and larger scavenging last time, that improves the mass flow rate of the intake port.

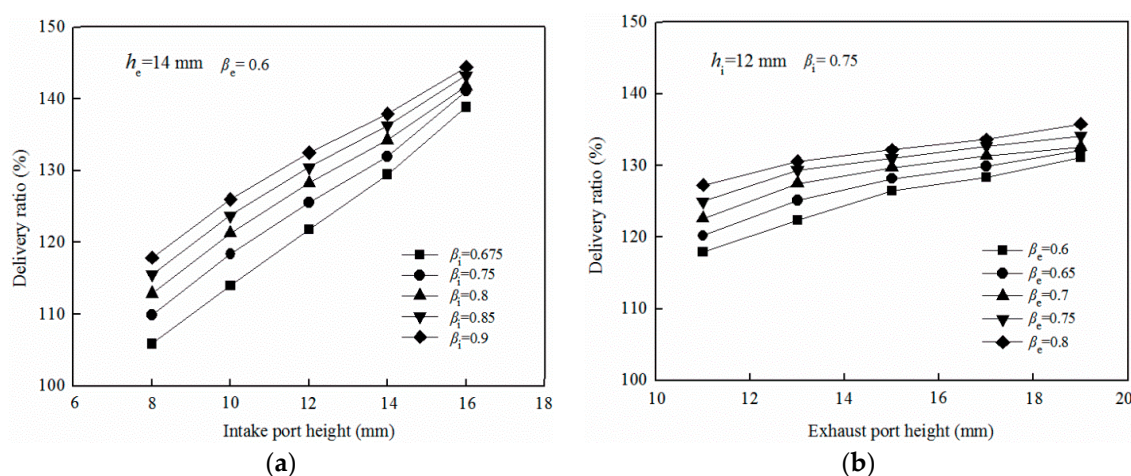


Figure 9. Effect of the port height and circumference ratio on delivery ratio (a) Intake port; (b) Exhaust port.

Delivery ratio also increases with the raise of the β_i ; for the β_i and scavenging area are proportional, which is positive for the intake mass flow rate. Figure 9b shows the effect of the h_e and β_e on delivery ratio. Delivery ratio increased with the raise of the h_e , because a higher h_e means an earlier EPO and larger free exhaust time resulting in lower cylinder pressure when the intake port was opened. Delivery ratio also increased with the raise of the β_e , because a larger exhaust area leads to a higher exhaust mass flow rate which results in a lower cylinder pressure when the intake port was opened. Considering Figure 9a,b, among the four impact factors, the h_i is the main factor affecting the engine delivery ratio.

Figure 10a shows the effect of the h_i and β_i on trapping efficiency, whereby the trapping efficiency decreased with the raise of the h_i ; the fresh air loss mass was increased when the h_i was raised, that all results in a larger scavenging duration time. Trapping efficiency also decreased with the raise of the β_i , because a larger β_i value leads to a larger scavenging port area, and when the scavenging area was raised, the mass flow rate of the intake and exhaust port were increased. However, the fresh air fraction in the exhaust gas was increased during the scavenging process; when the intake mass flow rate raised the loss of fresh air mass was increased too. Figure 10b shows the effect of the h_e and β_e on trapping efficiency, where the trapping efficiency decreased with the raise of the h_e , as a larger h_e means a longer exhaust port opening time which leads to more fresh air loss. Trapping efficiency also decreased with the raise of the β_e , because a larger β_e leads to a larger exhaust port area, which also leads to a high exhaust flow rate and air loss. Considering Figures 10a,b, among the four impact factors, the h_e is the main factor affecting the engine trapping ratio.

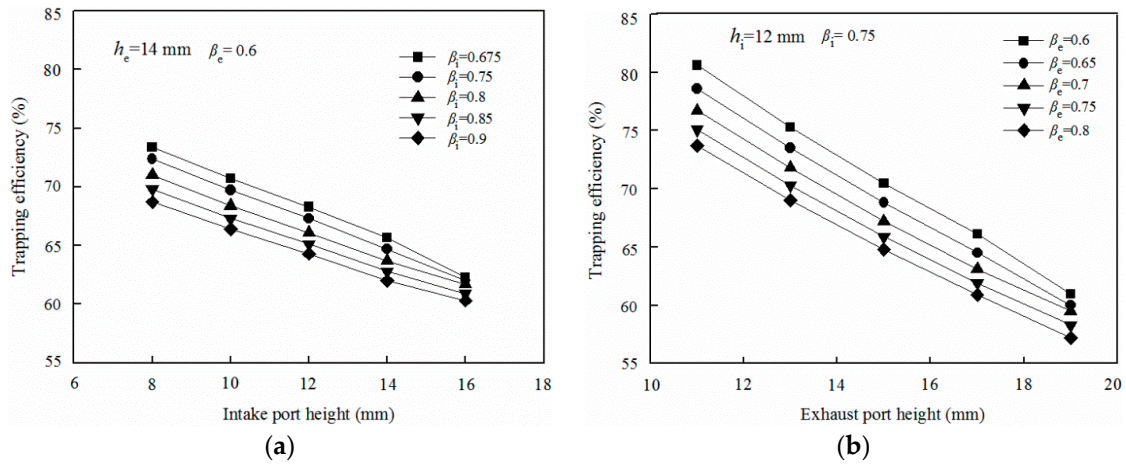
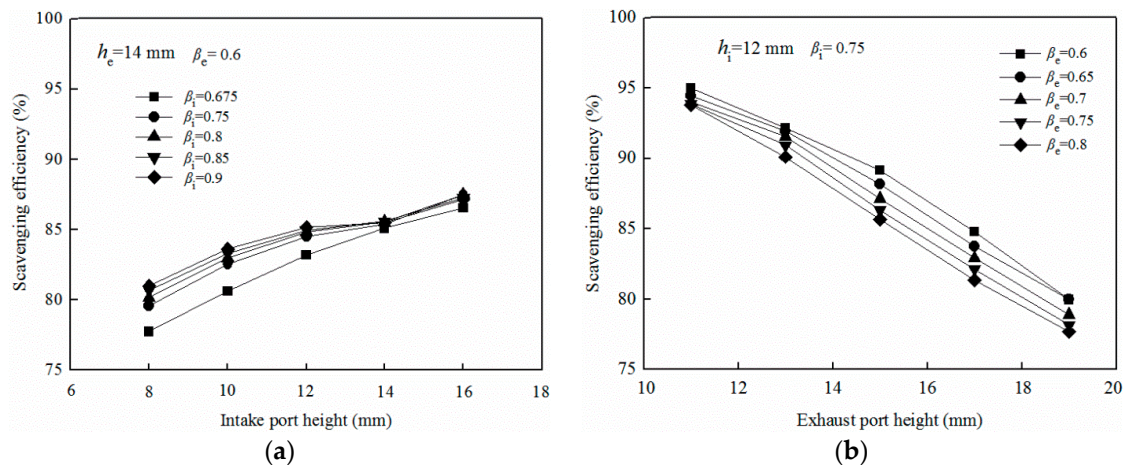


Figure 10. Effect of the port height and circumference ratio on trapping efficiency (a) Intake port; (b) Exhaust port.

Figure 11a shows the effect of the h_i and β_i on scavenging efficiency. When the h_i less than 14 mm, scavenging efficiency decreased with the raise of the h_i and β_e . The reason is that a larger h_i leads to a longer gas exchange time, and a larger β_e leads to a larger port area, and both these factors can raise the fresh air loss flow. When the h_i is larger than 14 mm, the β_e change has little effect on the scavenging efficiency. Figure 11b shows the effect of the h_e and β_e on scavenging efficiency. Scavenging efficiency also decreased with the raise of the h_e and β_e . The reason is same to that of the intake port, whereby a larger h_e leads to a longer gas exchange time, and a larger β_e leads to a larger port area, and the two factors result in a larger air loss flow. Contrasting Figure 11a,b, h_e is the main reason effecting the scavenging efficiency among the four impact factors.

For the uniflow scavenging system, the intake port was closed later than the exhaust port; the h_i defines the effective compression ratio. The exhaust port was opened earlier than the intake port, which means the h_e defines the effective expansion ratio. For a conventional engine the effective expansion ratio is the main factor defining the engine efficiency. OP2S-GDI engines also obey the same rule. Figure 12a shows the effect of the h_i and β_i on the indicated thermal efficiency and effective compression ratio, and it is not hard to summarize that h_i has a linear effect on the effective compression ratio but little effect on the indicated thermal efficiency. Figure 12b shows the effect of the h_e and β_e on the indicated thermal efficiency and effective expansion ratio. The h_e had a linear effect on the effective expansion ratio and decreased with the rise of the h_e , resulting in the indicated thermal efficiency also decreasing with the rise of the h_e . The β_e is another important factor affecting the indicated thermal efficiency. A β_e change leads to a variable cylinder pressure decay rate after EPO, so gas work on the piston would also be changed. The indicated thermal efficiency decreases with the rise of β_e . Comparing Figure 12a,b, the h_i affects the compression ratio while the h_e affects the expansion ratio, and the h_e is the main factor affecting the indicated thermal efficiency.



(a)

(b)

Figure 11. Effect of the port height and circumference ratio on scavenging efficiency (a) Intake port; (b) Exhaust port.

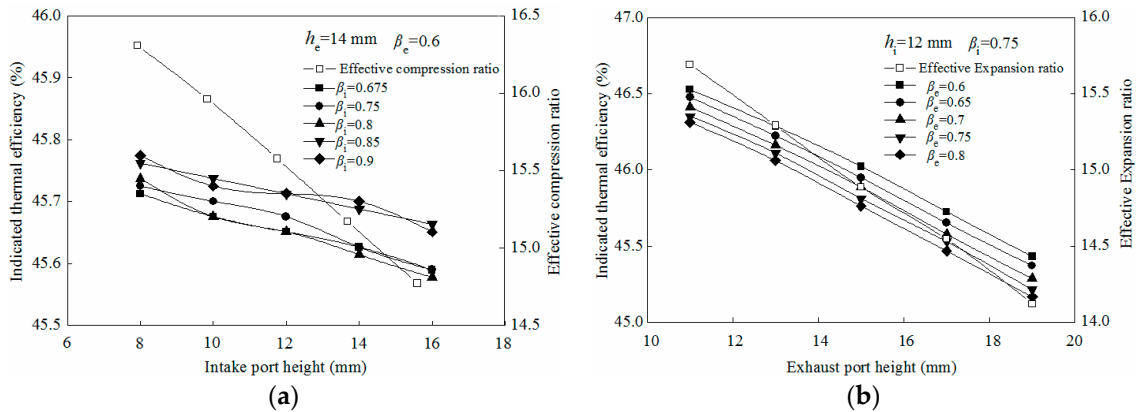


Figure 12. Effect of the port height and circumference ratio on working process (a) Intake port; (b) Exhaust port.

3.2.2. Orthogonal Experiment Schemes and Results

Scavenging process optimization is not just limited to the scavenging efficiency. Hofbauer [3] proposed using the engine speed characteristic as the optimization goal of the scavenging process. There is some fresh charge loss in the scavenging process, which cannot be reflected on the indicator diagram of the engine. The IMEP calculation should consider energy loss because of the fresh charge loss; at the same time, the work of the compressor for fresh charges should be included too.

At the end of the scavenging process, the volume of fresh charge in the cylinder is given by:

$$V_f = \eta_{sc} \cdot V_s \quad (12)$$

At every cycle, the work of the compressor for a fresh charge is given by:

$$W_c = (p_s - p_0) \cdot V_s \cdot \eta_{sc} \cdot l_0 \quad (13)$$

where p_s is scavenging pressure, p_0 is environment pressure, V_s is piston swept volume, l_0 is delivery ratio.

IMEP is given by:

$$p_i = \frac{W_i - W_c}{V_s} \quad (14)$$

where p_i is IMEP, W_i is the cycle net work.

The scavenging efficiency and cycle thermal efficiency can be taken into account simultaneously using IMEP as the optimized object of scavenging system parameters. When the IMEP is used as optimization goal, the optimization function is given by:

$$\text{MAX}(p_i) = f(\alpha_i, \alpha_e, \beta_i, \beta_e, \phi) \quad (15)$$

where α_i and α_e are the height stroke ratios of the intake and exhaust port, β_i and β_e are the circumference ratios of the intake and exhaust ports, ϕ is the opposed-piston motion phase difference.

Considering the comparability between different calculation cases, air-fuel ratio is selected as a constraint condition. Because the height stroke ratio of the intake and exhaust ports have a positive influence on the scavenging efficiency and a negative influence on the compression ratio, expansion ratio and cycle thermal efficiency, indicated specific fuel consumption is also selected as a constraint condition. The constraint condition is shown as follows:

$$s.t. : \begin{cases} a = 18 \\ b_i \leq 276 \text{ g/kW} \cdot \text{h} \end{cases} \quad (16)$$

where a is air-fuel ratio, b_i is the indicated specific fuel consumption.

An orthogonal experiment was employed as an optimizer tool. There are three levels and four factors in the calculations. Interactions between A and B, A and C, C and D will be considered, so the degrees of freedom are $5 \times 2 + 3 \times 2 \times 2 = 22$, so the calculation degrees of freedom must be more than 22, $L_{27}(3^{13})$ was employed in this calculation. Under the condition of full load at 6000 rpm, the calculation case is shown in Table 2.

Table 2. Calculation scheme and result.

No.	A		B		C		D		E		η_i (%)	l_o (%)	η_{tr} (%)	η_{sc} (%)	IMEP (bar)
	α_i (-)	β_i (-)	α_e (-)	β_e (-)	ϕ (°CA)										
1	0.1	0.7	0.123	0.6	5	45.7	96.3	90.5	87.2	12.31					
2	0.1	0.7	0.132	0.65	8.5	44.4	100.4	86.7	87.0	12.48					
3	0.1	0.7	0.141	0.7	12	42.5	104.1	84.3	87.8	12.53					
4	0.1	0.75	0.123	0.65	8.5	44.7	99.4	90.4	89.9	12.77					
5	0.1	0.75	0.132	0.7	12	42.8	101.9	87.2	88.8	12.64					
6	0.1	0.75	0.141	0.6	5	44.5	104.9	84.3	88.4	12.72					
7	0.1	0.8	0.123	0.7	12	43.1	99.2	90.8	90.1	12.65					
8	0.1	0.8	0.132	0.6	5	45.5	105.1	82.8	87.0	12.36					
9	0.1	0.8	0.141	0.65	8.5	44.1	108.1	79.5	85.9	12.35					
10	0.11	0.7	0.123	0.6	8.5	44.5	99.7	91.4	91.1	12.64					
11	0.11	0.7	0.132	0.65	12	42.7	101.2	87.7	88.7	12.33					
12	0.11	0.7	0.141	0.7	5	45	113.3	73.3	83.0	11.8					
13	0.11	0.75	0.123	0.65	12	43	98.8	90.7	89.6	12.33					
14	0.11	0.75	0.132	0.7	5	45.2	113.2	77.4	87.6	12.29					
15	0.11	0.75	0.141	0.6	8.5	44	109.4	79.9	87.4	12.32					
16	0.11	0.8	0.123	0.7	5	45.4	111.9	81.7	91.4	12.71					
17	0.11	0.8	0.132	0.6	8.5	44.3	107.6	83.9	90.2	12.62					
18	0.11	0.8	0.141	0.65	12	42.4	108.8	80.6	87.6	12.25					
19	0.12	0.7	0.123	0.6	12	42.8	97.5	91.3	89.0	12					
20	0.12	0.7	0.132	0.65	5	45	114.3	78.4	89.6	12.34					
21	0.12	0.7	0.141	0.7	8.5	43.7	116.1	74.9	86.9	12.22					
22	0.12	0.75	0.123	0.65	5	45.2	112.4	82.4	92.6	12.68					
23	0.12	0.75	0.132	0.7	8.5	44	114.5	78.3	89.6	12.38					
24	0.12	0.75	0.141	0.6	12	42.3	107.5	80.9	86.9	11.87					
25	0.12	0.8	0.123	0.7	8.5	44.2	111.4	82.4	91.7	12.54					
26	0.12	0.8	0.132	0.6	12	42.6	104.5	84.1	87.8	11.89					
27	0.12	0.8	0.141	0.65	5	44.8	122.4	71.1	87.0	12.04					

As the ϕ increases, a continuous drop is detected in the scavenging duration, resulting in a decreasing delivery ratio yet a rising trapping efficiency and an improvement in scavenging efficiency. Delivery ratio increases with the increasing α and β of the intake and exhaust ports; trapping efficiency falls as the α and β of the intake and exhaust ports increase; a positive correlation is found between scavenging efficiency and the α_i and β_i , while a negative correlation exists between scavenging efficiency and the α_e and β_e .

IMEP increases first and then decreases with an increasing ϕ . For effective compression ratio, it declines when the α_i goes up while for effective expansion ratio, it descends as the α_e increases. Such changes on the one hand reduce the IMEP value when the actual engine compression ratio declines with an increasing α_i , on the other hand it increases the IMEP value due to a large fresh charge input and fuel injection which is caused by the expanding scavenging area at the same crank angle as the β_i increases. When the β_i increases, the effect of α_i on IMEP gradually reduces and such influence is

particular obvious at the α_i of 0.9. When the α_e grows, the actual engine expansion ratio drops while IMEP shows a negative correlation with the increasing α_e when the α_i remains stable. With an increase of β_e , fresh charge storage is weakened and pressure drops during free exhaust, resulting in a lower IMEP due to a weakened effect of the burnt gas on the pistons.

3.2.3. Orthogonal Optimization Analysis

Correlation Analysis

The method of correlation analysis is employed to evaluate the correlation between key parameters and the evaluation index of the scavenging process. The absolute value of the correlation coefficient is less than or equal to 1. If the correlation coefficient is greater than 0 it is a positive correlativity; whereas otherwise it is a negative correlativity. The correlation varies with the correlation coefficient as follows:

$$\begin{array}{ll}
 \text{strongest correlation} & \text{for } |R| \geq 0.8 \\
 \text{strong correlation} & \text{for } 0.6 \leq |R| < 0.8 \\
 \text{moderate correlation} & \text{for } 0.4 \leq |R| < 0.6 \\
 \text{weak correlation} & \text{for } 0.2 \leq |R| < 0.4 \\
 \text{weakest correlation or no correlation} & \text{for } |R| < 0.2
 \end{array} \quad (17)$$

Based on Table 2, the correlation coefficient between the key parameters and the evaluation index of the scavenging process can be calculated, which is shown in Table 3. The α_i and α_e are the main influence factors for the delivery ratio and trapping efficiency, respectively. It is notable that the scavenging efficiency is primarily influenced by the α_e instead of α_i . As a key factor, the ϕ greatly affects the engine indicated thermal efficiency while the α_i has a great impact on the indicated mean effective pressure (IMEP).

Table 3. Correlation coefficient.

Parameter	α_i (-)	β_i (-)	α_e (-)	β_e (-)	ϕ (°)
l_0	0.541	0.241	0.453	0.354	-0.469
η_{tr}	-0.413	-0.169	-0.649	-0.304	0.437
η_{sc}	0.205	0.189	-0.687	0.041	0.058
η_i	-0.112	0.004	-0.22	-0.012	-0.915
IMEP	-0.463	0.124	-0.411	0.167	-0.124

Range Analysis

Based on Table 2, the mean values of 1, 2 and 3 can be obtained by summing for index values of the same level in the column including each factor, and the range value of this factor can be calculated, so as to determine the primary and secondary order of each factor, which is shown in Table 4. The range analysis results show that:

- (1) The effect order of various factors on the delivery ratio is $A > E > C > D > B > C \times D > \text{Error} > A \times C > A \times B$. Associating with correlation analysis, the α_i is the first factor for the delivery ratio.
- (2) The effect order of various factors on the trapping efficiency is $C > E > A > D > B > C \times D > A \times C > A \times B > \text{Error}$. Associating with correlation analysis, the α_e is the first factor for the trapping efficiency.
- (3) The effect order of various factors on the scavenging efficiency is $C > A > A \times B > D > A \times C > E > \text{Error} > C \times D > B$. Associating with correlation analysis, the α_e is the first factor for the scavenging efficiency.
- (4) The effect order of various factors on the indicated heat efficiency is $E > C > A > A \times C > B > A \times B > D > C \times D > \text{Error}$. Associating with correlation analysis, the ϕ is the first factor for the indicated heat efficiency.

- (5) The effect order of various factors on the IMEP is $A > C > E > B > \text{Error} > A \times B > C \times D > A \times C$. Associating with correlation analysis, the α_i is the first factor for the IMEP.

Table 4. Range analysis.

Parameter	A	B	A × B	C	A × C	D	E	C × D	Error	
l_0	Mean 1	102.16	104.77	106.89	102.96	106.81	103.61	110.42	105.85	106.596
	Mean 2	107.1	106.89	106.73	106.97	106.89	107.31	107.4	106.79	106.43
	Mean 3	111.18	108.78	106.82	110.51	106.73	109.51	102.61	107.8	107.40
	Range	9.022	4.011	0.3725	7.555	0.378	5.9	7.811	2.128	0.978
η_{tr}	Mean 1	0.863	0.843	0.8315	0.88	0.83	0.855	0.802	0.8365	0.832
	Mean 2	0.83	0.835	0.8355	0.829	0.83	0.831	0.83	0.8355	0.832
	Mean 3	0.804	0.819	0.8295	0.788	0.8365	0.811	0.864	0.8245	0.832
	Range	0.059	0.024	0.006	0.092	0.007	0.044	0.062	0.015	0.0057
η_{sc}	Mean 1	88.015	88.941	88.549	90.297	88.726	88.365	89.328	88.586	88.79
	Mean 2	89.662	89.003	89.384	88.525	88.919	88.684	88.896	89.03	88.98
	Mean 3	89.059	88.792	88.804	87.915	89.091	89.687	88.513	89.12	88.97
	Range	1.647	0.211	1.413	2.382	0.8985	1.322	0.815	0.714	0.749
η_i	Mean 1	44.144	44.033	44.033	44.289	44.056	44.022	45.144	44.033	44.011
	Mean 2	44.056	43.967	43.967	44.056	44.0385	44.033	44.211	43.962	44
	Mean 3	43.844	44.044	44.044	43.7	43.95	43.989	42.689	44.05	44.033
	Range	0.3	0.077	0.077	0.589	0.106	0.044	2.455	0.0885	0.074
IMEP	Mean 1	12.534	12.294	12.3645	12.514	12.3225	12.303	12.361	12.308	12.35867
	Mean 2	12.366	12.444	12.424	12.37	12.3535	12.397	12.48	12.442	12.33333
	Mean 3	12.218	12.379	12.329	12.233	12.4415	12.418	12.277	12.3675	12.42567
	Range	0.316	0.15	0.1395	0.281	0.1205	0.115	0.203	0.134	0.144

Variance Analysis

Based on Table 4, the significance level value of each factor can be calculated, which are shown in Table 5. If $F > F_{0.01}$, it is most significant, denoted by “****”; if $F_{0.01} \geq F > F_{0.05}$, it is more significant, denoted by “***”; if $F_{0.01} \geq F > F_{0.05}$, it is significant one, denoted by “**”. The variance analysis results show that:

- (1) The α_i , α_e , β_e and ϕ have most significant influence on the delivery ratio and the β_i has more significant influence on the delivery ratio.
- (2) All factors have no influence on the trapping efficiency.
- (3) The α_i , α_e and interaction of α_i and β_i have a significant influence on scavenging efficiency.
- (4) The α_i , α_e and ϕ have very significant influence on the indicated heat efficiency and interactions have no important influence on the indicated heat efficiency.
- (5) The α_i has a significant influence on IMEP and interactions have no significant influence on IMEP.

Table 5. Significance level.

Parameter	A	B	A × B	C	A × C	D	E	C × D	Error
l_0	***	**		***		***	***		
η_{tr}									
η_{sc}	*		**	**					
η_i	***			***			***		
IMEP	*								

***: $F > F_{0.01}$; **: $F_{0.01} \geq F > F_{0.05}$; *: $F_{0.01} \geq F > F_{0.05}$.

3.3. Optimization Results

The scavenging efficiency and cycle thermal efficiency can be taken into account simultaneously using IMEP as the optimized object of the scavenging system parameters. The

detailed results are shown in Table 2 and Figure 13. The α_i and β_i are 0.1 and 0.75, respectively; the α_e and β_e are 0.123 and 0.7, respectively; the ϕ is 17 °CA, therefore the optimal solution should be A1B2C1D3E2.

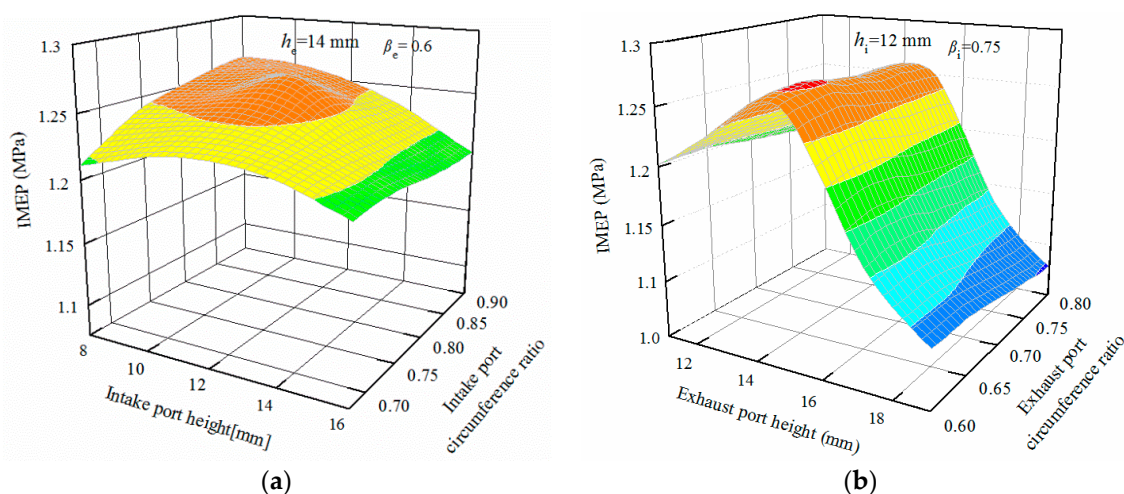


Figure 13. Effect of the port height and circumference ratio on IMEP (a) Intake port; (b) Exhaust port.

According to the results shown in Table 2, maximum scavenging efficiency means maximum IMEP. As shown in Figure 14, when the β_i and β_e are 0.75 and 0.6, the α_i and α_e have an optimal result for IMEP.

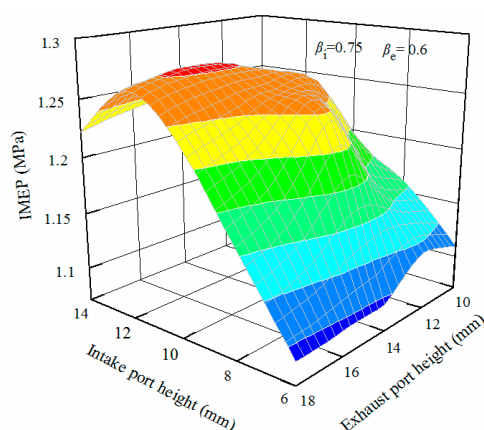


Figure 14. Effect of the intake and exhaust port height on IMEP.

For the OP2S-GDI engine, on the one hand port height is positive for gas exchange quality; on the other hand, port height is negative for engine indicated thermal efficiency. However, both high scavenging efficiency and high indicated thermal efficiency are positive for IMEP. IMEP can combine the parameter impacts on scavenging efficiency and indicated thermal efficiency, and it can be used as the optimization objective of the optimization function.

Table 4 shows the orthogonal calculation result on IMEP, it is easy to notice that:

$$\text{Max (IMEP)} = f(0.75, 0.6, 12, 14, 17) = 1.21 \text{ MPa}$$

While the $\text{Max}(\eta_{sc}) = f(0.85, 0.65, 13, 13, 17) = 93.4\%$. Table 6 shows the engine performance with optimum scavenging system parameters, all the parameters meet the constraint function. For the GDI engine, the fuel consumption has a minimum value when the air-fuel ratio is 18. When the air is more, the fuel can burn adequately [35]. The stratified mixture shortens the combustion duration so as to improve the thermal efficiency.

Table 6. OP2S-GDI engine performance with optimum scavenging system parameters.

Parameter	A/F	l_0 (%)	η_{tr} (%)	b_i (g/kW·h)
Value	18	116	76.9	276.7

4. Conclusions

A new optimization function was established using IMEP as the optimization objective. The effects of the different scavenging parameters on delivery ratio, trapping efficiency, and scavenging efficiency were studied; an orthogonal experiment was employed in the calculation process. The results of this analysis indicate that:

- (1) IMEP was employed to describe the effect of the scavenging system parameters on the engine performance more comprehensively than scavenging efficiency of the OP2S-GDI engine.
- (2) The h_i is the main factor affecting the engine delivery ratio, while the h_e is the main factor effect on the engine trapping ratio, scavenging efficiency and indicated thermal efficiency.
- (3) The h_e is the most important factor affecting the gas exchange process of OP2S-GDI engine.

Acknowledgments: The authors gratefully acknowledge the financial support by the National Natural Science Foundation of China (Grant No. 51605447), the Applied Basic Research Programs of Shanxi Province in China (Grant No. 201601D021085) and the National Ministry Fundamental Research Foundation of China (Grant No. B2220110005).

Author Contributions: Fu-Kang Ma and Jun Wang designed the orthogonal experiment; Yan-Gang Zhang and Yao-Nan Fen performed the simulation; Yi Zhang and Yu-Hang Liu analyzed the data; Fu-Kang Ma and Tie-Xiong Su contributed to the editing and reviewing of the document.

Conflicts of Interest: The authors declare no conflict of interest.

Nomenclature

Abbreviations

1D	mono-dimensional
3D	three-dimensional
CFD	computational fluid dynamics
EPO	exhaust port opening
GDI	gasoline direct injection
IDC	inner dead center
IMEP	indicated mean effective pressure
IPC	intake ports closing
IPO	intake ports opening
ISFC	indicated specific fuel consumption
ODC	outer dead center
OP2S	opposed-piston two-stroke
OPOC	opposed piston opposed cylinder
TDC	top dead center

Symbols

a	A/F ratio
b_i	indicated specific fuel consumption
d	port width
d_i	intake port width,
d_e	exhaust port width
F_s	port area function
h	port height
h_i	intake port height

h_e	exhaust port height
l_0	delivery ratio
n	engine speed
p_s	inlet pressure
p	cylinder pressure
p_z	export pressure
V_s	cylinder displacement volume
V_f	volume of fresh charge
α	height stroke ratio
α_i	intake port height stroke ratio
α_e	exhaust port height stroke ratio
β	port circumference ratio
β_i	intake port circumference ratio
β_e	exhaust port circumference ratio
ϕ	opposed-piston phase difference
μ_s	intake port discharge coefficient
η_{sc}	scavenging efficiency
η_{tr}	trapping efficiency

References

- Callahan, B.J.; Wahl, M.H.; Froelund, K. Oil consumption measurements for a modern opposed-piston two-stroke diesel engine. In Proceedings of the ASME 2011 Internal Combustion Engine Division Fall Technical Conference, Morgantown, WV, USA, 2–5 October 2011; pp. 1019–1028.
- Kalebjian, C.; Redon, F.; Wahl, M. Low emissions and rapid catalyst light-off capability for upcoming emissions regulations with an opposed-piston, two-stroke diesel engine. In Proceedings of the Emissions Conference, Ypsilanti, MI, USA, 12–13 June 2012.
- Hofbauer, P. *Opposed Piston Opposed Cylinder (OPOC) Engine for Military Ground Vehicles*; SAE International: Warrendale, PA, USA, 2005.
- Hirsch, N.R.; Schwarz, E.E.; McGough, M.G. *Advanced Opposed-Piston Two-Stroke Diesel Demonstrator*; SAE International: Warrendale, PA, USA, 2006.
- Herold, R.E.; Wahl, M.H.; Regne, G. *Thermodynamic Benefits of Opposed-Piston Two-Stroke Engines*; SAE International: Warrendale, PA, USA, 2011.
- McGough, M.G.; Rd U.; Ctr E. *Experimental Investigation of the Scavenging Performance of a Two-Stroke Opposed-Piston Diesel Tank Engine*; SAE International: Warrendale, PA, USA, 2004.
- Franke, M.; Huang, H.; Liu, J.P. *Opposed Piston Opposed Cylinder (OPOC™) 450 hp Engine: Performance Development by CAE Simulations and Testing*; SAE International: Warrendale, PA, USA, 2006.
- Regner, G.; Herold, R.; Wahi, M. The Achatas Power Opposed-Piston Two-Stroke Engine: Performance and Emissions Results in a Medium-Duty Application. *Int. J. Engines* **2011**, *4*, 2726–2735.
- Xu, S.; Wang, Y.; Zhu, T.; Xu, S.; Wang, Y.; Zhu, T.; Xu, T.; Tao, C. Numerical analysis of two-stroke free piston engine operating on HCCI combustion. *Appl. Energy* **2011**, *88*, 3712–3725.
- Xu, H.; Song, J.; Yao, C.; Xu, H.J.; Song, J.O.; Yao, C.D.; Liu, C.Z.; Yu, H.S.; Hao, Y.G.; Wang, Q.X. Simulation on In-Cylinder Flow on Mixture Formation and Combustion in OPOC Engine. *Trans. CSICE* **2009**, *27*, 395–400.
- Chen, W.; Zhuge, W.; Zhang, Y.; Yu, H.S. Simulation on the scavenging process of the opposite two-stroke diesel engine. *J. Aerosp. Power* **2010**, *25*, 1322–1326.
- Zhao, F.; Lai, M.C.; Harrington, D.L. Automotive spark-ignited direct-injection gasoline engines. *Prog. Energy Combust.* **1999**, *25*, 437–562.
- Arcoumanis, C.; Bae, C.; Hu, Z. *Flow and Combustion in a Four Valve, Spark-Ignition Optical Engines*; SAE International: Warrendale, PA, USA, 1994.
- Fan, L.; Reitz, R.D.; Trigui, N. *Intake Flow Simulation and Comparison with PTV Measurements*; SAE Technical : New York, NY, USA, 1999.
- Wu, J. Similar design method used on the port size on the two-stroke diesel engine. *Trans. Eng. Thermophys.* **1981**, *2*, 145–153.

16. Liu, Y. A Modification to the “Fully Mixed/Layers Formed” compound scavenging model in a two-stroke diesel engine with Constant Pressure Charging. *Intern. Combust. Engine Eng.* **1985**, *4*, 33–41.
17. Zhao, F. *Simulation Analysis and Optimization on the Scavenging Process for the Uniflow-Scavenge Diesel Engine*; Dalian University of Technology: Dalian, China, 2010.
18. Ma, F.; Zhao, C.; Zhang, F.; Zhao, Z.; Zhang, Z. An Experimental Investigation on Combustion and Heat Release Characteristics of an Opposed-Piston Folded-Cranktrain Diesel Engine. *Energies* **2015**, *8*, 6365–6381.
19. He, C.; Xu, S. *Transient Gas Exchange Simulation and Uniflow Scavenging Analysis for a Unique Opposed Piston Diesel Engine*; SAE International: Warrendale, PA, USA, 2016.
20. Wang, X.; Ma, J.; Zhao, H. *Evaluations of Scavenge Port Designs for a Boosted Uniflow Scavenged Direct Injection Gasoline (BUSDIG) Engine by 3D CFD Simulations*; SAE International: Warrendale, PA, USA, 2016.
21. Ma, J.; Zhao, H. *The Modeling and Design of a Boosted Uniflow Scavenged Direct Injection Gasoline (BUSDIG) Engine*; SAE International: Warrendale, PA, USA, 2015.
22. Zhang, Y.; DallaNora, M.; Zhao, H. *Investigation of Valve Timings on Lean Boost CAI Operation in a Two-stroke Poppet Valve DI Engine*; SAE International: Warrendale, PA, USA, 2015.
23. Ma, J.; Zhao, H.; Freeland, P.; Hawley, M.; Xia, J. Numerical Analysis of a Downsized 2-Stroke Uniflow Engine. *SAE Int. J. Engines* **2014**, *7*, 2035–2044.
24. Regner, G.; Johnson, D.; Koszewnik, J. *Modernizing the Opposed Piston, Two Stroke Engine for Clean, Efficient Transportation*; SAE International: Warrendale, PA, USA, 2014.
25. Mattarelli, E.; Rinaldini, C.A.; Cantore, G. *2-Stroke Externally Scavenged Engines for Range Extender Applications*; SAE International: Warrendale, PA, USA, 2012.
26. Krishna, A.S.; Mallikarjuna, J.M.; Kumar, D. Effect of engine parameters on in-cylinder flows in a two-stroke gasoline direct injection engine. *Appl. Energy* **2016**, *176*, 282–294.
27. Carlucci, A.P.; Ficarella, A.; Trullo, G. Performance optimization of a Two-Stroke supercharged diesel engine for aircraft propulsion. *Energy Convers. Manag.* **2016**, *122*, 279–289.
28. Carlucci, A.P.; Ficarella, A.; Laforgia, D.; Renna, A. Supercharging system behavior for high altitude operation of an aircraft 2-stroke Diesel engine. *Energy Convers. Manag.* **2015**, *101*, 470–480.
29. Ma, F.; Zhao, C.; Zhang, F.; Zhao, Z.; Zhang, S. Effects of Scavenging System Configuration on In-cylinder Air Flow Organization of an Opposed-Piston Two-Stroke Engine. *Energies* **2015**, *8*, 5866–5884.
30. Willcox, M.; Cleaves, J.; Jackson, S.; Hawkes, M.; Raimond, J. *Indicated Cycle Efficiency Improvements of a 4-Stroke, High Compression Ratio, S.I., Opposed-Piston, Sleeve-Valve Engine Using Highly Delayed Spark Timing for Knock Mitigation*; SAE International: Warrendale, PA, USA, 2012.
31. Ma, F.; Zhao, C.; Zhao, Z.; Zhang, S. Scavenge Flow Analysis of Opposed-Piston Two-Stroke Engine Based on Dynamic Characteristics. *Adv. Mech. Eng.* **2015**, *7*, 1–11.
32. Taylor, C.F. *The Internal-Combustion Engine in Theory and Practice: Thermodynamics, Fluid Flow, Performance*, 2nd ed.; MIT Press: Cambridge, UK, 1985.
33. Gamma Technologies, Engine Performance Application Manual, GT-Powerv.7.1. Available on line <http://www.gtisoft.com/>. (accessed on 19 December 2016)
34. Sigurdsson, E.; Ingvorsen, K.M.; Jensen, M.V. Numerical analysis of the scavenge flow and convective heat transfer in large two-stroke marine diesel engines. *Appl. Energy* **2014**, *123*, 37–46.
35. Bai, Y.; Wang, Z.; Wang, J. Part-load characteristics of direct injection spark ignition engine using exhaust gas trap. *Appl. Energy* **2010**, *87*, 2640–2646.

